NeuroImage 90 (2014) 280–289

Contents lists available at ScienceDirect

NeuroImage

journal homepage: www.elsevier.com/locate/ynimg

Structural neuroimaging correlates of allelic variation of the BDNF val66met polymorphism

Natalie J. Forde [a,*,1], Lisa Ronan [b,1], John Suckling [b,d,h], Cathy Scanlon [a], Simon Neary [a], Laurena Holleran [a], Alexander Leemans [c], Roger Tait [d], Catarina Rua [b], Paul C. Fletcher [b,d,h], Ben Jeurissen [e], Chris M. Dodds [f], Sam R. Miller [f], Edward T. Bullmore [b,d,f,h], Colm McDonald [a], Pradeep J. Nathan [b,f,g], Dara M. Cannon [a]

[a] Clinical Neuroimaging Laboratory, School of Medicine, College of Medicine, Nursing and Health Sciences, National University of Ireland Galway, Galway, Ireland
[b] Brain mapping unit, Department of Psychiatry, University of Cambridge, Cambridge, UK
[c] Image Sciences Institute University Medical Center Utrecht, The Netherlands
[d] Behavioural and Clinical Neuroscience Institute, Department of Experimental Psychology, University of Cambridge, Cambridge, UK
[e] iMinds Vision Lab, University of Antwerp, Belgium
[f] GlaxoSmithKline, Clinical Unit Cambridge, UK
[g] School of Psychology and Psychiatry, Monash University, Australia
[h] Cambridge and Peterborough NHS Foundation Trust, Cambridge, UK

ARTICLE INFO

Article history:
Accepted 16 December 2013
Available online 31 December 2013

Keywords:
BDNF
Structural
Diffusion
MRI
Val66met
Intrinsic curvature

ABSTRACT

Background: The brain-derived neurotrophic factor (BDNF) val66met polymorphism is associated with altered activity dependent secretion of BDNF and a variable influence on brain morphology and cognition. Although a met-dose effect is generally assumed, to date the paucity of met-homozygotes have limited our understanding of the role of the met-allele on brain structure.
Methods: To investigate this phenomenon, we recruited sixty normal healthy subjects, twenty in each genotypic group (val/val, val/met and met/met). Global and local morphology were assessed using voxel based morphometry and surface reconstruction methods. White matter organisation was also investigated using tract-based spatial statistics and constrained spherical deconvolution tractography.
Results: Morphological analysis revealed an "inverted-U" shaped profile of cortical changes, with val/met heterozygotes most different relative to the two homozygous groups. These results were evident at a global and local level as well as in tractography analysis of white matter fibre bundles.
Conclusion: In contrast to our expectations, we found no evidence of a linear met-dose effect on brain structure, rather our results support the view that the heterozygotic BDNF val66met genotype is associated with cortical morphology that is more distinct from the BDNF val66met homozygotes. These results may prove significant in furthering our understanding of the role of the BDNF met-allele in disorders such as Alzheimer's disease and depression.

Introduction

Brain-derived neurotrophic factor (BDNF) is a secretory protein from the neurotrophin family which is vital for the survival, maintenance, differentiation and morphology of neurons (e.g. Cohen-Cory and Fraser, 1995). It is essential for neuronal plasticity which is fundamental to both early and late long term potentiation (Pang and Lu, 2004). A common single nucleotide polymorphism (SNP) occurs in the 5′ proBDNF domain at nucleotide 196 (dbSNP number rs6265), of guanine to adenine, resulting in a valine (val) to methionine (met)

Abbreviations: BDNF, brain derived neurotrophic factor; val, valine; met, methionine; AD, Alzheimer's Disease; MDD, Major depressive disorder; NAA, n-acetyl-asparate; VBM, voxel-based morphometry; CSD, constrained spherical deconvolution; EPI, echo planar imaging; DW, diffusion weighted; FOD, fibre orientation distribution; ILF, inferior longitudinal fasciculus; CB, cingulum bundle; UF, uncinate fasciculus; FA, fractional anisotropy; GLM, general linear model; TBSS, tract-based spatial statistics; ANCOVA, analysis of co-variance; TFCE, threshold-free cluster enhancement; ICC, intraclass correlation; SD, standard deviation; SNP, single nucleotide polymorphism.

* Corresponding author at: Clinical Neuroimaging Laboratory, 202 Comerford Suite, Clinical Sciences Institute, NUI Galway, Ireland.
E-mail addresses: j.natalieforde@gmail.com (N.J. Forde), lr344@cam.ac.uk (L. Ronan), js369@cam.ac.uk (J. Suckling), cathy.scanlon@nuigalway.ie (C. Scanlon), s.neary2@nuigalway.ie (S. Neary), l.holleran1@nuigalway.ie (L. Holleran), Alexander@isi.uu.nl (A. Leemans), Rt337@cam.ac.uk (R. Tait), cr439@cam.ac.uk (C. Rua), pcf22@cam.ac.uk (P.C. Fletcher), Ben.jeurissen@ua.ac.be (B. Jeurissen), Chrismdodds@googlemail.com (C.M. Dodds), sam.r.miller@gsk.com (S.R. Miller), etb23@cam.ac.uk (E.T. Bullmore), colm.mcdonald@nuigalway.ie (C. McDonald), pn254@cam.ac.uk (P.J. Nathan), dara.cannon@nuigalway.ie (D.M. Cannon).
[1] Joint first author.

1053-8119
http://dx.doi.org/10.1016/j.neuroimage.2013.12.050

amino acid substitution at codon 66 (val66met). This SNP is present in approximately 36%, (3% homozygous), of the Caucasian population with a higher incidence in Asian populations (Consortium, 2003).

The BDNF met-allele has been associated with memory impairments (Kambeitz et al., 2012) and multiple neurological and psychiatric conditions including Alzheimer's disease (AD, Matsushita et al., 2005; Ventriglia et al., 2002). A significant number of studies have investigated the link between BDNF and anxiety, particularly in relation to depression (MDD, Frodl et al., 2007; Verhagen et al., 2010). Some studies have indicated that the met/met variant is associated with increased anxiety (Chen et al., 2006; Montag et al., 2010a), though other studies have reported contradictory findings (Lang et al., 2005; Sen et al., 2003).

Although the val66met polymorphism does not seem to affect the activity of mature BDNF, the intracellular trafficking and activity-dependent secretion of BDNF is altered (Egan et al., 2003). At a cellular level, there appears to be a met-dose effect on intracellular localisation (Chen et al., 2004) and regulation of activity-dependent secretion of BDNF (Chen et al., 2006). Variations in n-acetyl-aspartate (NAA) levels in the hippocampus associated with the met-allele also suggest a functional met-dose effect (Egan et al., 2003).

Whether these findings are correlated with similar met-dose effects on brain structure has not been investigated thoroughly due to a dearth of met-homozygotes in the population. Instead, the majority of studies have concatenated met-carriers to investigate the effects of the val66met BDNF polymorphism rather than the specific met-dose effect. Of these studies, a significant number have focused on hippocampal volumetry (Bueller et al., 2006; Frodl et al., 2007; Szeszko et al., 2005; Takahashi et al., 2008). However the effect size of met-related volume reductions in the hippocampii is small and findings are heterogeneous. Moreover, meta-analysis has raised the possibility that these findings have been subject to a "winner's curse" rather than a genuine biological effect of the allele (Molendijk et al., 2012). In whole-brain analyses, the met-allele has been associated with GM reductions in the bilateral dorsolateral prefrontal cortex (Pezawas et al., 2004), right thalamus, amygdala and fusiform gyrus (Montag et al., 2009), parahippocampal gyrus (Montag et al., 2009; Takahashi et al., 2008), and total occipital and temporal GM volume (Toro et al., 2009). However results are conflicting (Eker et al., 2005), and some studies have found no differences between groups (Frodl et al., 2007; Joffe et al., 2009).

Relatively fewer studies have examined the effects of the val66met polymorphism on white matter (WM) microstructural organisation in healthy individuals (Carballedo et al., 2012; Chiang et al., 2011; Kennedy et al., 2009; Montag et al., 2010b; Soliman et al., 2010; Tost et al., 2013; Voineskos et al., 2011). One of the largest diffusion-MRI studies to date ($n = 455$, $n = 21$ met/met) reported increased fractional anisotropy (FA) associated with the met-allele in several white matter tract areas including the splenium of the corpus callosum, fornix and left inferior longitudinal fasciculus (ILF) (Chiang et al., 2011). The remaining studies had few if any met-homozygotes and the findings are inconsistent. For example, while one study reported reduced FA bilaterally in the uncinate fasciculus amongst met-carriers (Soliman et al., 2010), others have reported increases in FA associated with the met-allele (Carballedo et al., 2012; Chiang et al., 2011; Tost et al., 2013). Several other studies have failed to find any effect of genotype on brain structure (Kennedy et al., 2009; Montag et al., 2010b; Voineskos et al., 2011). Most recently, increased FA in the left anterior cingulum bundle was found in met-carriers (Carballedo et al., 2012).using deterministic tensor-based tractography. Additionally increased FA has been found in several clusters amongst met-carriers including portions of the splenium and body of the corpus callosum, the posterior thalamic radiation, posterior and bilateral superior corona radiata, the right internal capsule and the superior longitudinal fasciculus (Tost et al., 2013).

In summary, there is a significant lack of convergence in analyses of the BDNF val66met polymorphism on brain structure. Over and above differences in sample sizes and methodology, it may be that the variation in the relative proportions of hetrozygous and homozygous met-carriers which are often concatenated within the same sample group may contribute to these inconsistencies. However, without a quantitative analysis of the met-dose effect, the relative contribution of this variation is unknown. To date no such study has been undertaken.

The aim of this study was to distinguish between the effects of met-homozygotes, heterozygotes and val-homozygotes on brain structure by recruiting balanced genetic groups. Given the heterogeneity of previous analysis, we proposed to use a quartet of complementary approaches to determine the structural correlates of each genotype. In the first instance, because BDNF is widely expressed in the brain (Binder and Scharfman, 2004), and has been shown to affect cortical morphology (Montag et al., 2009; Pezawas et al., 2004), we employed a global morphological parameter, namely cortical intrinsic curvature (Ronan et al., 2011, 2013) which is a function of the differential expansion of the surface during development, and may be related to the underlying architecture and connectivity of the cortex. Intrinsic curvature is mathematically more fundamental to a surface than folding, and has been demonstrated to be more sensitive to case–control differences than measures of gyrification (Ronan et al., 2012).

We further employed voxel-based morphometry (VBM) which is specifically designed to obviate global size and shape differences for the purpose of identifying regional changes between groups (Good et al., 2001). Furthermore we employed the recent tractography method of constrained spherical deconvolution (CSD) to assess, sub-cortical white matter organisation (Jeurissen et al., 2011). CSD holds significant advantages over previously used tensor-based models in its ability to estimate multiple contributing fibre orientations within a voxel, making the reconstruction of fibre bundles in areas of crossing fibres possible (Tournier et al., 2007). We also utilised the automated restricted voxelwise method of tract-based spatial statistics (TBSS, Smith et al., 2006) to investigate diffusion throughout the core white matter tracts of the brain at a voxel level to compliment the tract specific tractography analysis.

By combining these complimentary approaches and with the novelty of a large met-homozygous group we aimed to more fully characterise the changes in brain structure associated with the val66met polymorphism of BDNF.

Methodology

Participants

Healthy subjects, prospectively genotyped for the BDNF val66met gene polymorphism, were recruited from a database of approx 11,000 subjects at the Phase I GSK Clinical Unit and the Cambridge BioResource, Cambridge Biomedical Research Centre (CBRC). Of these approx. 350 had the rare met/met polymorphism. Information letters were sent to those on the database about the study and those that responded and fulfilled our exclusion/inclusion criteria were then included in a smaller database. Inclusion criteria included being right-handed, male or female, age 18–55 years and of a healthy weight ($\geq$50 kg men, $\geq$40 kg female and able to fit comfortably into scanner). Exclusion criteria included having a medical condition which could potentially affect the studies goals; neurological disorders including learning disability/disorder, family history of epilepsy, history of alcohol or drug abuse within the previous 6 months, history of Axis I psychiatric disorders, smokers, positive test results for HIV, Hep B or Hep C, use of prescription or non-prescription drugs including vitamins, herbal or dietary supplements within 7 days of screening. This smaller database included approx. 25 met/met subjects. From this database, subjects were prospectively recruited into 3 groups (20 val/val; 20 val/met and 20 met/met) in a randomised and blinded manner such that the recruitment team and the experimentors were blinded to the genotype. One person in the team (not involved in recruitment or analysis) was unblinded such that equal number of subjects were included in the groups matched for age, gender and IQ. Subjects were also asked to refrain from caffeine and alcohol intake 24 h prior to and on

the day of testing. Written informed consent was obtained from all participants. Ethical approval for this study was received from the National Research Ethics Service (NRES) committee East of England — Cambridge South. This study comprised part of larger study of various behavioural, neuroimaging, neuropsychometric and neurophysiological assessment of the BDNF polymorphism in human behaviour.

Genotyping

DNA was extracted from blood samples via standard methods and genotyped for the BDNF Val66Met SNP via TaqMan 50exonuclease assay (Applied Biosystems, Foster City, CA, USA).

Morphometric analysis

MRI data acquisition

MR images were acquired on a 3 T Siemens TimTrio at the Wolfson Brain Imaging Centre, University of Cambridge. Structural data were acquired with a sagittal MPRAGE T1-weighted, three-dimensional, inversion recovery gradient echo sequence with the following parameters: Inversion time = 900 ms; echo time = 2.98 ms; repetition time = 2300 ms flip angle = 9°; voxel dimensions = 1 mm × 1 mm × 1 mm. Acquisition time = 9.14 min.

A 2D interleaved axial diffusion echo planar imaging (EPI) sequence was applied for the diffusion data acquisition where 63 diffusion gradient directions were used with b = 1000 s/mm^2 and one B_0 reference image was acquired with the following parameters: TE = 90 ms, TR = 7800 ms, FOV = 192 mm, matrix = 192 × 192, slice thickness 2 mm, voxel dimension = 2 mm × 2 mm × 2 mm. Acquisition time = 8.44 min.

Morphometric analysis

We use multiple methods of analysis. For intrinsic curvature we use the skew of the distribution as a global metric. Both VBM and TBSS are voxel-based methods where analysis between groups is done in a voxel by voxel manner. In tractography the median FA is extracted from the isolated tracts for analysis.

Global analysis: intrinsic curvature

Cortical reconstructions were generated using FreeSurfer (Dale et al., 1999; Fischl and Dale, 2000; Fischl et al., 1999a,b). The FreeSurfer programme was specifically developed for cortical reconstruction. In brief, raw image data voxels were sub-sampled to voxels of size 1 mm^3. After that the data were normalized for intensity. RF-bias field inhomogenieties were modelled and removed, followed by skull-stripping. The cerebral white matter was subsequently identified after which the hemispheres were separated, tessellated and deformed to produce an accurate and smooth representation of the grey-white interface. Reconstructions were edited manually, where inaccuracies occurred. These edits were made on two-dimensional slices though the reconstruction and hence may be considered to be effectively unbiased with respect to the morphological parameters which are three-dimensional.

The software Caret (v5.65, http://brainmap.wustl.edu/caret) was used to calculate cortical intrinsic curvature per vertex of each subject's FreeSurfer-reconstruction. This process has been detailed elsewhere (Ronan et al., 2013). Intrinsic curvature arises from the differential expansion of the cortical surface, such that regions with a greater degree of differential expansion have a greater degree of intrinsic curvature. Because expansion is mediated by the underlying regional cytoarchitecture, intrinsic curvature is taken as a proxy of this (Ronan et al., 2011, 2013). Once generated in Caret, the derived surface curvature files were subsequently imported to MatLab where a low-pass filter was applied to remove aberrantly high curvature values that were not compatible with the resolution of the cortical reconstruction (Ronan et al., 2012, 2013). For each subject, the value per vertex contributed to the distribution of all values across the cortex for that subject, from which the skew was calculated. Cortical intrinsic curvature has a heavily skewed distribution (Pienaar et al., 2008; Ronan et al., 2011, 2012). As brain size changes, this distribution changes both its mean value as well as its shape (Ronan et al., 2012, 2013). Because we are interested in the degree of curvature independent of head size, we calculated the skew of the distribution rather than its mean.

Regional analysis: VBM

Structural data was analysed with FSL-VBM (Douaud et al., 2007 http://fsl.fmrib.ox.ac.uk/fsl/fslwiki/FSLVBM), an optimised VBM protocol (Good et al., 2001), carried out with FSL tools (Smith et al., 2004).

Images were reoriented to standard space, brain-extracted and grey matter-segmented before being aligned to the MNI 152 template (Andersson et al., 2007). MNI 152 alignment involved affine registration of grey matter images to GM ICBM-152 to create a first pass affine template; non-linear re-registration of native grey matter images to the affine template was then performed. Resulting warped images were averaged and reflected along the mid-line to create a left-right symmetric, study-specific grey matter template in MNI 152 space. To avoid bias in the form of favouring one group over another during registration, all subjects were included in the template construction process.

All native images were non-linearly registered to the study-specific template and modulated to correct for local expansion and contraction due to the non-linear component of the spatial transformation. Modulation was achieved by multiplication of each voxel of each registered image by the Jacobian of the associated warp field. Finally, modulated grey matter images were smoothed with an isotropic Gaussian kernel with a sigma of 3 mm. At each step, quality and error identification was determined visually using data rendered into a web browser. No images were rejected in this process.

TBSS and tractography

Diffusion MRI data processing and analyses

Diffusion-weighted (DW) images were corrected for eddy current induced geometric and motion distortions, including rotation of the B-matrix (Leemans and Jones, 2009), using the graphical toolbox ExploreDTI v4.8.2 (Leemans et al., 2009). Tensor estimation was performed by non-linear robust estimation of tensors by outlier rejection, RESTORE, (Chang et al., 2005). Data quality was determined visually including steps outlined previously (Tournier et al., 2011). No images were rejected in this process. T1-weighted structural MR images were corrected for non-uniform bias using N3 (Sled et al., 1998), brain extraction performed using the FSL brain extraction tool BET (Smith, 2002) and finally registered to the corrected FA diffusion images using the FSL's linear registration tool FLIRT (Jenkinson and Smith, 2001).

TBSS

Voxel-by-voxel based statistical analysis was carried out on the corrected FA data using Tract Based Spatial Statistics, TBSS (Smith et al., 2006). Briefly all FA images were non-linearly aligned to the target FMRIB58_FA standard space image then affine transformed to MNI152 1 mm^3 standard space. These images were merged and averaged to generate a study specific mean FA image and FA skeleton preparation using an FA threshold of 0.2.

Tractography

Whole brain deterministic tractography using CSD (Tournier et al., 2007) with interpolation of the fibre orientation distribution (FOD) was performed in ExploreDTI v4.8.2 (Jeurissen et al., 2011; Leemans et al., 2009). The following parameters were applied: maximum spherical harmonic order for CSD 8, seed point resolution 2 × 2 × 2 mm^3, step size 1 mm, angle threshold 40 and 45 depending on tract anatomy and fibre length range 50–500 mm. Tracts were selected for analysis based upon their previous implication in the literature (Carballedo et al., 2012; Chiang et al., 2011; Kennedy et al., 2009; Montag et al., 2010b;

Soliman et al., 2010; Tost et al., 2013; Voineskos et al., 2011) and biological connection to diseases associated with the met66val allele: the splenium of the corpus callosum, inferior longitudinal fasciculus (ILF, 45), fornix, cingulum bundle (CB; dorsal and anterior), arcuate fasciculus (AF) and uncinate fasciculus (UF, 40). To avoid bias all regions were drawn on the structural T1 images, registered to the FA.

For anatomical tract definition, the splenium of the corpus callosum, UF, AF and ILF were isolated following a modified version of Wakana et al. (2007) protocols. Dorsal and anterior CB's were defined similarly to a previous study (Carballedo et al., 2012) and the fornix was isolated with a single coronal gate at its apex. Segments of tracts used for subsequent analysis are shown in Fig. 1 and lie between the gates indicated in green. (For details of anatomical tract definition see supplementary information).

Statistical analyses

Statistical analyses were carried out in IBM SPSS statistics 20 unless otherwise stated. The Chi-squared test was used to assess gender balance across genotype-groups. The Shapiro–Wilks test and Levene's test were used to determine normality of distribution and homogeneity of variance respectively for median FA of the tracts, intrinsic curvature, extracted grey matter volumes and age. A one-way ANOVA was employed to compare age between groups. A three-level one-way univariate analysis of co-variance (ANCOVA) was employed for all analyses, so as to be unbiased in our approach and fully utilise having 3 balanced genotype groups.

Intrinsic curvature analysis

Group differences in intrinsic curvature skew were tested using an ANCOVA with whole brain surface area, hemisphere, age and gender as covariates. Post-hoc Bonferroni-corrected pairwise comparisons, with the same covariates, followed significant findings.

Voxel-based morphometric analysis

Grey matter voxel-wise GLM statistical analysis of the 3 groups was performed using CamBA v2.3.0 (http://www-bmu.psychiatry.cam.ac.uk) with gender, age and total intracranial volume as covariates.

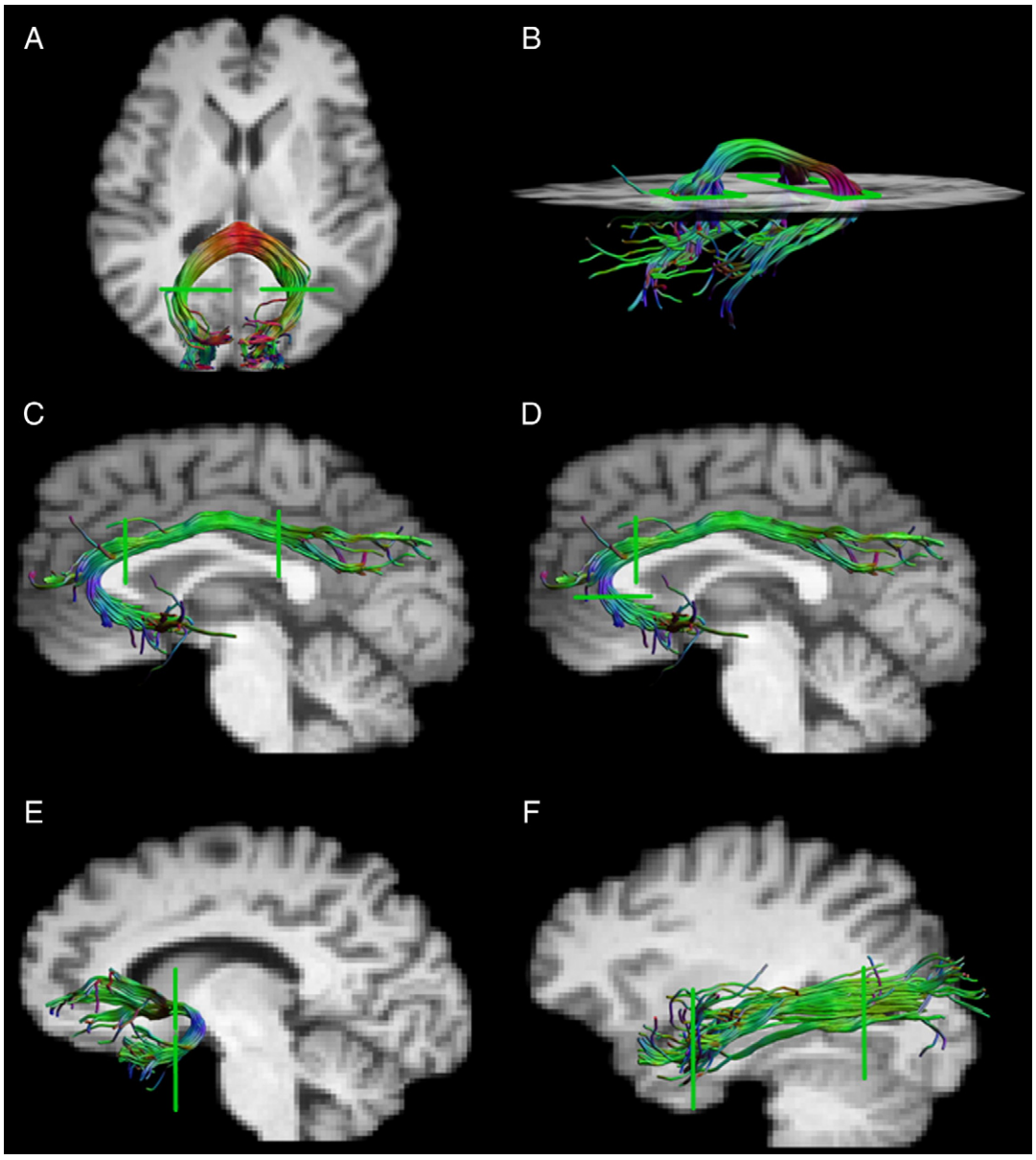

Fig. 1. Reconstructed white matter tracts superimposed on T1-MRI for anatomical reference. Green lines indicate the extent of the segments included in analyses. (A) Splenium of the corpus callosum, (B) fornix, (C) dorsal cingulum bundle, (D) anterior cingulum bundle, (E) uncinate fasciculus and (F) inferior longitudinal fasciculus.

Statistical inference was by permutation analysis on voxel clusters, with a statistical threshold corrected such that the expected number of false positive clusters in the intracranial volume was <1 (Bullmore et al., 1999). The location of significant clusters was established in relation to the anatomical automatic labelling (AAL) atlas in MNI standard space (Tzourio-Mazoyer et al., 2002). Post-hoc Bonferroni-corrected pairwise comparisons, with the same covariates, followed on the volumes extracted from significant clusters.

TBSS analysis and tractography

For TBSS voxel-wise GLM statistical analysis along the skeleton was performed using randomise, part of the FSL programme, with age and gender as covariates. This involved permutation analysis (10,000 random) and threshold-free cluster enhancement (TFCE) to correct for multiple comparisons (Behrens et al., 2007; Nichols and Holmes, 2002).

For tractography, segments of tracts were analysed to minimise variability in tract length allowing adjusted tract volume (tract volume/median tract length) to be used as a covariate (Vos et al., 2011), along with age and gender in an ANCOVA to compare median FA between groups. Post-hoc Bonferroni-corrected pairwise comparisons, with the same covariates, followed for tracts with significant findings.

Cross modality testing

Secondary to significant findings in the primary analysis we investigated the presence of links between these findings from the different modalities by correlation analysis (Pearson correlation).

Results

Demographics

Groups did not differ significantly in gender proportion or mean age (Table 1). One met/met subject was not available for the curvature analysis, however this did not result in any demographic differences between the groups in terms of age ($F_{(2)} = 0.84$, $p = 0.43$) or gender ($\chi^2 = 24$, $p = 0.58$). Similarly DW data was not available for one member of the val/met group, this did not affect the age ($F_{(2)} = 0.48$, $p = 0.62$) or gender ($\chi^2_{(2)} = 0.77$, $p = 0.71$) balance between groups.

Intrinsic curvature

A main effect of group was found on the intrinsic curvature skew ($F_{(2)} = 10.29$, $p < 001$, adj. $R^2 = 0.31$). The mean intrinsic curvature skew for each group was as follows: met/met 5.48 ± 0.14; val/met 5.38 ± 0.18; val/val 5.53 ± 0.19. Post-hoc Bonferroni-corrected pairwise comparisons revealed a significantly smaller intrinsic curvature skew in the val/met group compared to the val/val group ($F_{(1)} = 16.00$, $p < 0.001$, adj. $R^2 = 0.28$, Fig. 2A) and a non-significant trend towards reduction compared to the met/met group ($F_{(1)} = 6.02$, $p = 0.05$, adj. $R^2 = 0.28$). There was no statistically significant difference between the met/met and val/val groups, although there was a non-significant trend ($F_{(1)} = 5.35$, $p = 0.07$, adj. $R^2 = 0.27$).

Table 1
Participant demographic variables.

Demographic variable	BDNF genotype			Group comparison	
	met/met	val/met	val/val	Test statistic	p value
n	20	20	20		
Age, mean (SD)	42.2 (9.7)	40.9 (10.1)	39.0 (11.2)	$F = 0.50$	0.61
Age, range	20–55	24–55	19–54		
Sex (male/female)	10/10	15/5	14/6	$\chi^2 = 0.52$	0.77

Voxel-based morphometry

Voxel-wise analysis revealed 3 significant regions of group differences in grey matter volume following thresholding at the cluster level; 1) cerebellum, 2) cerebellum/fusiform and 3) right superior frontal/supplementary motor area (see Table 2 and Fig. 3). In each case the val/met group showed either significantly larger (or trends towards significantly larger) values than both other groups, while there was no statistically significant difference between the homozygous groups resulting in a "U-shaped profile" (Table 2, Fig. 3).

TBSS and tractography

TBSS failed to detect clusters that survived correction for multiple comparisons across genotype-groups.

The single rater's (NJF) intra-rater reliability was greater than 86% in defining tracts (ICC range 0.86–0.99). Median FA outliers were defined as lying outside the mean ± 3 times the SD. One right UF and two splenium tracts were removed on this basis which did not affect mean age or gender balance between the groups (right UF: age, $F_{(2)} = 0.60$, $p = 0.55$; gender, $\chi^2_{(2)} = 0.79$, $p = 0.68$; splenium: age, $F_{(2)} = 0.84$, $p = 0.44$; gender, $\chi^2_{(2)} = 0.34$, $p = 0.85$).

Statistical analysis found a significant effect of group in the right dorsal CB (Table 3, Fig. 2B). No other significant effects were observed in the remaining tracts examined, a trend was seen in the splenium of the corpus callosum (Table 3). Subsequent post-hoc Bonferroni-corrected pairwise analysis of the right dorsal CB revealed the overall group difference to be driven by the met/met group having a significantly lower FA than the val/met group (Table 3, Fig. 2B), the other comparisons showed no statistically significant difference between groups (Table 3).

Correlations

No significant relationship was detected between morphometric GM differences, white matter anisotropy or intrinsic curvature. A correlation was seen between the intrinsic curvature skew and the GM volume of cluster 3, however this was not significant following correction (Pearson correlation −0.26, $p = 0.046$, uncorrected).

Discussion

This is the first comprehensive study of the effect of met-homozygosity and heterozygosity on grey and white matter morphometry. Such analyses are rare and offer a key insight into the effects of the BDNF val66met polymorphism. Our results indicate a global and local effect of genotype on cortical morphology and white matter organisation. However, contrary to our expectations we found no evidence to support a met-dose effect in any of the modalities used herein. Instead we found that the met-allele has a significant but non-uniform effect on brain structure, with homozygotes (met/met and val/val) more similar than heterozygotes (val/met) across all our findings irrespective of modality.

To date the majority of structural investigations in BDNF have focused on regional effects, despite the fact that the gene is expressed globally (Binder and Scharfman, 2004). Our results indicate that BDNF has a global effect on cortical morphology in line with previous analyses (Toro et al., 2009).

In our global analysis of cortical morphology, the results of intrinsic curvature analysis indicate that a single copy of the met-allele is associated with a modest decrease in curvature skew, which in turn may be interpreted as an increase in the degree of intrinsic curvature and hence differential expansion (the degree of non-uniform expansion). Previous experiments and theoretical considerations have related the degree of differential expansion to neuronal density, with regions of higher density reducing the degree of cortical differential expansion owing to a proportionately greater degree of tangential pressure

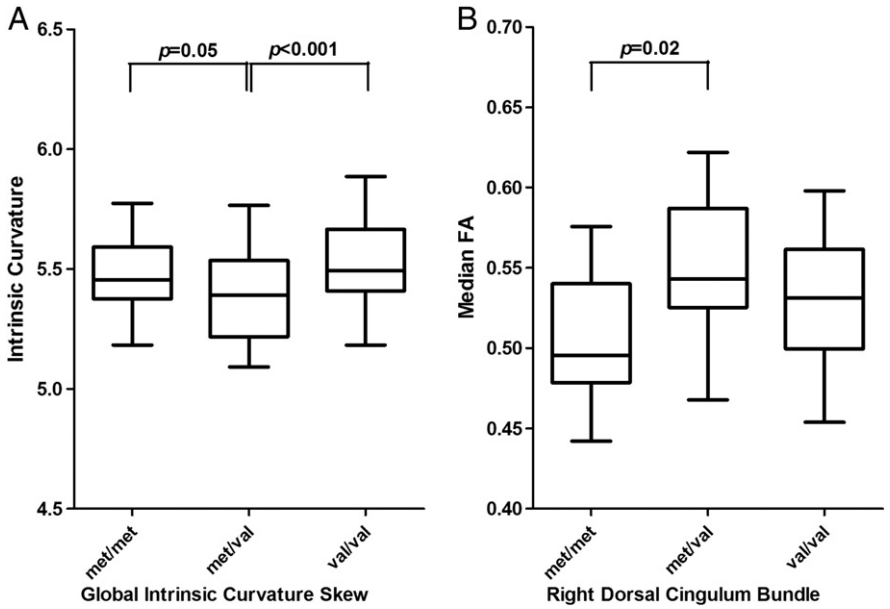

Fig. 2. Intrinsic curvature and anisotropy. A significant effect of genotype was seen on intrinsic curvature skew (A) and on the FA in the right dorsal cingulum bundle (B). Post-hoc analysis revealed that val/met has a significantly smaller intrinsic curvature than val/val. Also there is a significant reduction in FA in the met/met group when compared to val/met in the right dorsal cingulum bundle. Box plots with interquartile range and median line. Whiskers represent max and min values.

under expansion which acts to reduce spatial variance (Ronan et al., 2011, 2013). In turn neuronal density has been demonstrated to have a reciprocal relationship with local connectivity, where higher densities are related to a decrease in synaptic connectivity and dendritic aborisation (Cullen et al., 2010; Schlaug et al., 1993; Welker, 1990). Based on this rationale, we may tentatively interpret the decrease in intrinsic curvature skew as reflecting a change in the intrinsic structure of the cortex, possibly reflecting decreased neuronal density and associated changes in intrinsic connectivity. At one level these results are in agreement with the wider literature, where BDNF has been demonstrated to be influential in the density of neurons (Gorski et al., 2003) and the formation, maintenance and modulation of connectivity (Cao et al., 2007; Horch et al., 1999; McAllister et al., 1997). However there is a paucity of studies on the specific met-dose effect on these changes. Moreover these effects are often observed to be layer-specific (Gorski et al., 2003; McAllister et al., 1997) making it difficult to reconcile these observations with the results reported herein which are based on the tangential morphology of the cortex which is insensitive to such radial variations.

Local effects were also uncovered both in grey matter volume and white matter organisation. We have shown 3 clusters of genotypic difference in grey matter volume. The first two are mainly constrained to the cerebellum but also include voxels in lingual areas bilaterally. The third is unilateral on the right side including areas of the superior and middle frontal areas and supplementary motor area. Adequately comparing these regional difference findings to the literature is somewhat of a challenge as the whole brain is usually neglected in favour of analyses focussed on the hippocampus. However our cluster in the right fusiform gyrus does correspond to a previous finding of reduced volume amongst met-carriers in this area (Montag et al., 2009). In the same study right frontal regions were also implicated, but these regions do not overlap directly with our right frontal cluster but do support our findings in laterality and adjacent regions affected (Montag et al., 2009). Hippocampal investigations in BDNF are legion, and most commonly

Table 2
Summary of VBM clusters.

	Extent (voxels)	Lobe	Regions (AAL atlas)
Cluster 1	958	Cerebellum	Cerebellum (crus2_R, 7b_R, 8_R)
Cluster 2	1551	Frontal	Lingual (R, L)
		Temporal	Fusiform R
		Parietal	Cerebellum (crus1R, 4_5L, 4_5R, 6 L, 6R, 9R)
		Cerebellum	Vermis (4_5, 6, 9 10)
Cluster 3	886	Frontal	Frontal (SupR, MidR)
		Parietal	Precentral R
			Supp motor area R

Post hoc

		met/met v val/met	met/met v val/val	val/met v val/val
Cluster 1	$F_{(1)}$	6.73	2.40	13.93
	p	0.09	1.00	0.006**
	adj. R^2	0.11	0.07	0.25
Cluster 2	$F_{(1)}$	20.33	3.27	28.31
	p	<0.001***	0.71	<0.001***
	adj. R^2	0.44	0.15	0.48
Cluster 3	$F_{(1)}$	15.07	0.44	19.58
	p	0.004**	1.00	<0.001***
	adj. R^2	0.29	0.10	0.32

***p < 0.001, **p < 0.01.

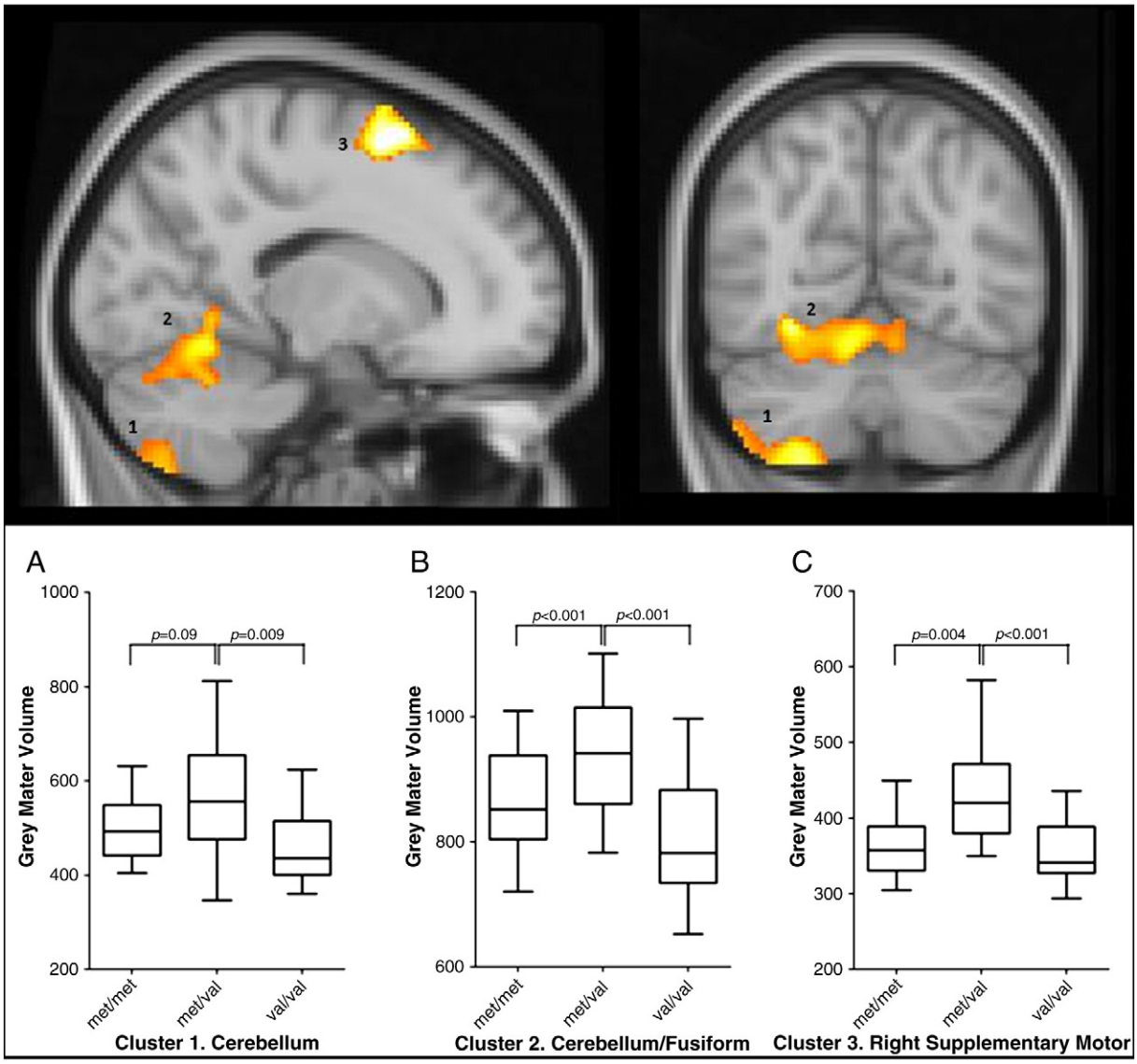

Fig. 3. Voxel-based morphometry. Three clusters of significant group effect were found in the grey matter VBM analysis. These clusters are highlighted in the image above and detailed in the table. Graphs indicate the differences in the GM volume between the 3 genotypes within each cluster. Box plots with interquartile range and median line. Whiskers represent max and min values.

Table 3
Summary of tractography findings.

Tract	Mean FA (SD)			Test statistic ($F_{(2)}$)	p value
	met/met	val/met	val/val		
Dorsal CB right	0.51 (0.04)	0.55 (0.04)	0.53 (0.04)	3.50	0.04*
Dorsal CB left	0.57 (0.03)	0.58 (0.04)	0.59 (0.05)	0.04	0.96
Splenium	0.73 (0.03)	0.72 (0.03)	0.74 (0.02)	2.80	0.07
Fornix	0.33 (0.06)	0.31 (0.04)	0.31 (0.06)	1.39	0.26
ILF left	0.47 (0.02)	0.45 (0.03)	0.46 (0.03)	0.79	0.46
ILF right	0.43 (0.02)	0.43 (0.03)	0.43 (0.03)	0.32	0.73
Anterior CB left	0.42 (0.04)	0.43 (0.05)	0.43 (0.06)	0.42	0.66
Anterior CB right	0.39 (0.04)	0.41 (0.05)	0.41 (0.05)	2.03	0.14
Arcuate left	0.51 (0.03)	0.52 (0.02)	0.51 (0.04)	1.33	0.27
Arcuate right	0.43 (0.03)	0.44 (0.04)	0.44 (0.05)	0.19	0.83
Uncinate left	0.41 (0.04)	0.41 (0.04)	0.40 (0.04)	0.57	0.57
Uncinate right	0.39 (0.02)	0.41 (0.04)	0.39 (0.04)	1.07	0.35

Post hoc

		met/met v val/met	met/met v val/val	val/met v val/val
Dorsal CB right	$F_{(1)}$	8.37	1.20	1.31
	p	0.02*	0.84	0.26
	adj. R^2	0.14	0.04	−0.06

* $p < 0.05$.

indicate a met-effect of reduced hippocampal volume (Pezawas et al., 2004), although these changes are not consistent (Koolschijn et al., 2010; Toro et al., 2009), and have recently been suggested to be artificial due to a "winners curse" (Molendijk et al., 2012). In our analysis we did not detect an effect of genotype in the hippocampus.

A subtle local effect of genotype was found on the white matter organisation of the right dorsal cingulum bundle and this was found to be due to a statistically significantly higher FA amongst the heterozygotes compared to the met-homozygotes. Met-homozygotes have not previously been examined in the literature. However, there has been a report of increased FA in the left anterior and dorsal CB amongst val/met-heterozygotes relative to val-homozygotes (Carballedo et al., 2012). We did not observe differences between groups in white matter organisation across the left CB or any other tract examined which is largely consistent with the literature to date comparing met-carriers to val-homozygotes (Kennedy et al., 2009; Montag et al., 2010b; Voineskos et al., 2011). Previous inconsistency in the literature could largely be due to the mixing of met-homozygotes and heterozygotes when they may in fact have diverging effects on white matter microstructure relative to the val-homozygous group. Also anisotropy in all studies prior to the present analysis has depended upon tensor-based methods and may therefore be confounded by collapsing changes in multiple within-voxel compartments. The amount of white matter voxels that exhibit a configuration with multiple fibre populations has recently been estimated to be up to 90%, invalidating tensor based tractography approaches in large parts of the brain (Jeurissen et al., 2013). Spherical deconvolution based tractography, used here, deconvolves the diffusion signal into multiple estimated contributing compartments representing differently oriented bundles within each voxel and may therefore overcome the above mentioned potential confound. Our restricted voxel-based analysis (TBSS) failed to detect any difference in groups this may be due to limitations in the method of TBSS as well as the above mentioned confounds in using tensor based methods. These include the thinning of white matter tracts to a skeleton thereby reducing the amount of white matter examined and skeleton dys-contiguity where crossing tracts or tract junctions occur (Smith et al., 2006). This may account for the inconsistency across our diffusion findings.

Common across all our findings is the "U-shaped" profile, where heterozygotes are distinct from the homozygotes. Given our relative lack of insight in to the biology of the BDNF met-allele, as well as a dearth of studies examining the met-dose effect on brain structure, it is yet too early to know how to interpret these changes. However it does offer the important insight that, by grouping all met-carriers together, previous quantitative investigations may have missed an important aspect of the interaction between the met and val alleles. Although not explicitly discussed or statistically significant, several studies have indicated similar U-shaped trends in BDNF. Examples include prior to task-related activity but not after (Kleim et al., 2006), or in memory scores and NAA levels of schizophrenia patients and their siblings (Egan et al., 2003). However a number of studies have also indicated a predominance of met-dose effects of BDNF on cortical microstructure (Chen et al., 2004; Liu et al., 2012). Moreover, in a sister-study of the current analysis, a met-dominant effect was most likely in fMRI response (Dodds et al., 2013) as well as plasticity (using TMS, Teo et al., in press). While this may suggest that there is not a simple relationship between genotype and phenotype, it more importantly emphasises the importance of replication of our structural analysis. In general, the heterogeneity of structural findings, in terms of the pattern, and effect-size is, as Molendijk and colleagues point out, further enhanced by the paucity of studies which explicitly model the met-dose effect (Molendijk et al., 2012). The results of this study clearly indicate that further work is required to illuminate these global and regional effects.

Our findings suggest that the effect of the met allele is more strongly felt in the grey matter compared to the white. Significant group differences in the VBM analysis ranged in effect size from moderate to large (adj. $R^2 = 25–48\%$) while the significant finding in the right dorsal cingulum bundle corresponded to a small (14%) effect size. We see this as a true finding given the robust methods used and the similar pattern to the VBM and intrinsic curvature findings. Changes in FA can be very subtle and it is possible that our sensitivity to detect differences in FA may be limited by the methods employed and given a larger sample size effects of similar small size may have been detected in some other tracts, however this is speculative and we await the replication of this finding and the addition of more with the help of balanced groups as used herein. Alternatively, it remains possible that although BDNF is expressed throughout the brain, the val66met polymorphism may have its main effect at synapses in the grey matter where it is known to modulate the activity dependent secretion of BDNF (Egan et al., 2003). Further research shall determine this.

There are important limitations to this study. Recruiting participants for studies, such as this, where one of the groups is comprised of individuals with a rare genotype (met/met, 3%) can be exceedingly difficult. This was in part overcome by the prospective recruitment of participants from a large database of subjects of known genotype. Despite having a significantly larger number of met-homozygotes participate in this study than previous studies there remains a small risk that we may be missing a subtle effect of genotype that a larger study would have found. Gender by BDNF genotype interactions have been shown (Shalev et al., 2009; Verhagen et al., 2010) which may have confounded our findings as our val/met and val/val groups were more dominated by men, however we have minimised this risk by including gender as a covariate in all our analyses. The segmentation of tracts to account for partial volume effects is another potential confound (Vos et al., 2011), and it is possible that changes in peripheral tract regions were excluded from analysis. More generally there are multiple alleles upstream of the BDNF gene associated with the val66met polymorphism, which may contribute to the heterogeneity of results across the literature in a fundamental way (Okada et al., 2006) and thus obfuscate the true nature of the BDNF polymorphism in limited sample sizes such as the one we report. Similarly, epigenetic modulation of BDNF gene regulation may also confound results (Boulle et al., 2012).

Conclusion

In this study we explicitly examined the role of met-load in the BDNF val66met polymorphism on human cerebral grey and white matter morphometry. Our results indicate global and local changes associated with the met66 allele of BDNF which do not occur in a dose-dependent manner. Our findings of a non-linear pattern of genotypic effect illustrate the importance of classifying met-homozygous, heterozygous and val-homozygous subjects into separate groups to adequately determine the effect of the met-allele. Elucidating the role of variation in the gene coding for this cerebral neuronal growth factor is essential to ultimately understanding its potential as a risk factor or target in the treatment of depression.

Acknowledgments

We gratefully acknowledge the participation of all NIHR Cambridge BioResource and GSK Clinical Unit Panel volunteers. We thank staff of the CBR and GSK Clinical Unit for assistance with volunteer recruitment. We thank members of the Cambridge BioResource SAB and Management Committee for their support and the National Institute for Health Research Cambridge Biomedical Research Centre for funding.

Conflict of interest

This study was funded by GlaxoSmithKline. Chris M Dodds, Sam R Miller, Edward T Bullmore and Pradeep J Nathan are current or past employees of GlaxoSmithKline and hold shares in the company. Simon

Neary received the Irish Health Research Board summer student scholarship (www.hrb.ie). Lisa Ronan, Catarina Rua and Paul Fletcher were funded by the Bernard Wolfe Health Neuroscience Fund and by the Wellcome Trust.

Appendix A. Supplementary data

Supplementary data to this article can be found online at http://dx.doi.org/10.1016/j.neuroimage.2013.12.050.

References

Andersson, J.L.R., Jenkinson, M., Smith, S., 2007. Non-linear Registration aka Spatial Normalisation.

Behrens, T., Smith, S., Webster, M., Nichols, T., 2007. Randomise v2.1.

Binder, D.K., Scharfman, H.E., 2004. Brain-derived neurotrophic factor. Growth Factors 22, 123–131.

Boulle, F., van den Hove, D.L., Jakob, S.B., Rutten, B.P., Hamon, M., van Os, J., Lesch, K.P., Lanfumey, L., Steinbusch, H.W., Kenis, G., 2012. Epigenetic regulation of the BDNF gene: implications for psychiatric disorders. Mol. Psychiatry 17, 584–596.

Bueller, J.A., Aftab, M., Sen, S., Gomez-Hassan, D., Burmeister, M., Zubieta, J.K., 2006. BDNF Val66Met allele is associated with reduced hippocampal volume in healthy subjects. Biol. Psychiatry 59, 812–815.

Bullmore, E.T., Suckling, J., Overmeyer, S., Rabe-Hesketh, S., Taylor, E., Brammer, M.J., 1999. Global, voxel, and cluster tests, by theory and permutation, for a difference between two groups of structural MR images of the brain. IEEE Trans. Med. Imaging 18, 32–42.

Cao, L., Dhilla, A., Mukai, J., Blazeski, R., Lodovichi, C., Mason, C.A., Gogos, J.A., 2007. Genetic modulation of BDNF signaling affects the outcome of axonal competition in vivo. Curr. Biol. 17, 911–921.

Carballedo, A., Amico, F., Ugwu, I., Fagan, A.J., Fahey, C., Morris, D., Meaney, J.F., Leemans, A., Frodl, T., 2012. Reduced fractional anisotropy in the uncinate fasciculus in patients with major depression carrying the met-allele of the Val66Met brain-derived neurotrophic factor genotype. Am. J. Med. Genet. B Neuropsychiatr. Genet. 159B, 537–548.

Chang, L.C., Jones, D.K., Pierpaoli, C., 2005. RESTORE: robust estimation of tensors by outlier rejection. Magn. Reson. Med. 53, 1088–1095.

Chen, Z.Y., Patel, P.D., Sant, G., Meng, C.X., Teng, K.K., Hempstead, B.L., Lee, F.S., 2004. Variant brain-derived neurotrophic factor (BDNF) (Met66) alters the intracellular trafficking and activity-dependent secretion of wild-type BDNF in neurosecretory cells and cortical neurons. J. Neurosci. 24, 4401–4411.

Chen, Z.Y., Jing, D., Bath, K.G., Ieraci, A., Khan, T., Siao, C.J., Herrera, D.G., Toth, M., Yang, C., McEwen, B.S., Hempstead, B.L., Lee, F.S., 2006. Genetic variant BDNF (Val66Met) polymorphism alters anxiety-related behavior. Science 314, 140–143.

Chiang, M.C., Barysheva, M., Toga, A.W., Medland, S.E., Hansell, N.K., James, M.R., McMahon, K.L., de Zubicaray, G.I., Martin, N.G., Wright, M.J., Thompson, P.M., 2011. BDNF gene effects on brain circuitry replicated in 455 twins. Neuroimage 55, 448–454.

Cohen-Cory, S., Fraser, S.E., 1995. Effects of brain-derived neurotrophic factor on optic axon branching and remodelling in vivo. Nature 378, 192–196.

Consortium, T.I.H., 2003. The International HapMap Project. Nature 426, 789–796.

Cullen, D.K., Gilroy, M.E., Irons, H.R., Laplaca, M.C., 2010. Synapse-to-neuron ratio is inversely related to neuronal density in mature neuronal cultures. Brain Res. 1359, 44–55.

Dale, A.M., Fischl, B., Sereno, M.I., 1999. Cortical surface-based analysis. I. Segmentation and surface reconstruction. Neuroimage 9, 179–194.

Dodds, C.M., Henson, R.N., Suckling, J., Miskowiak, K.W., Ooi, C., Tait, R., Soltesz, F., Lawrence, P., Bentley, G., Maltby, K., Skeggs, A., Miller, S.R., McHugh, S., Bullmore, E.T., Nathan, P.J., 2013. Effects of the BDNF Val66Met polymorphism and met allele load on declarative memory related neural networks. PLoS One 8, e74133.

Douaud, G., Smith, S., Jenkinson, M., Behrens, T., Johansen-Berg, H., Vickers, J., James, S., Voets, N., Watkins, K., Matthews, P.M., James, A., 2007. Anatomically related grey and white matter abnormalities in adolescent-onset schizophrenia. Brain 130, 2375–2386.

Egan, M.F., Kojima, M., Callicott, J.H., Goldberg, T.E., Kolachana, B.S., Bertolino, A., Zaitsev, E., Gold, B., Goldman, D., Dean, M., Lu, B., Weinberger, D.R., 2003. The BDNF val66met polymorphism affects activity-dependent secretion of BDNF and human memory and hippocampal function. Cell 112, 257–269.

Eker, Ç., Kitis, Ö., Ozan, E., Okur, H., Eker, O.D., Ersoy, M.A., Akdeniz, F., Vahip, S., Akarsu, N., Gonul, A.S., 2005. BDNF gene val66met polymorphism associated grey matter changes in human brain bulletin of clinical. Psychopharmacology (Berl) 15.

Fischl, B., Dale, A.M., 2000. Measuring the thickness of the human cerebral cortex from magnetic resonance images. Proc. Natl. Acad. Sci. U. S. A. 97, 11050–11055.

Fischl, B., Sereno, M.I., Dale, A.M., 1999a. Cortical surface-based analysis. II: Inflation, flattening, and a surface-based coordinate system. Neuroimage 9, 195–207.

Fischl, B., Sereno, M.I., Tootell, R.B., Dale, A.M., 1999b. High-resolution intersubject averaging and a coordinate system for the cortical surface. Hum. Brain Mapp. 8, 272–284.

Frodl, T., Schule, C., Schmitt, G., Born, C., Baghai, T., Zill, P., Bottlender, R., Rupprecht, R., Bondy, B., Reiser, M., Moller, H.J., Meisenzahl, E.M., 2007. Association of the brain-derived neurotrophic factor Val66Met polymorphism with reduced hippocampal volumes in major depression. Arch. Gen. Psychiatry 64, 410–416.

Good, C.D., Johnsrude, I.S., Ashburner, J., Henson, R.N., Friston, K.J., Frackowiak, R.S., 2001. A voxel-based morphometric study of ageing in 465 normal adult human brains. Neuroimage 14, 21–36.

Gorski, J.A., Zeiler, S.R., Tamowski, S., Jones, K.R., 2003. Brain-derived neurotrophic factor is required for the maintenance of cortical dendrites. J. Neurosci. 23, 6856–6865.

Horch, H.W., Kruttgen, A., Portbury, S.D., Katz, L.C., 1999. Destabilization of cortical dendrites and spines by BDNF. Neuron 23, 353–364.

Jenkinson, M., Smith, S., 2001. A global optimisation method for robust affine registration of brain images. Med. Image Anal. 5, 143–156.

Jeurissen, B., Leemans, A., Jones, D.K., Tournier, J.D., Sijbers, J., 2011. Probabilistic fiber tracking using the residual bootstrap with constrained spherical deconvolution. Hum. Brain Mapp. 32, 461–479.

Jeurissen, B., Leemans, A., Tournier, J.D., Jones, D.K., Sijbers, J., 2013. Investigating the prevalence of complex fiber configurations in white matter tissue with diffusion magnetic resonance imaging. Hum. Brain Mapp. 34, 2747–2766.

Joffe, R.T., Gatt, J.M., Kemp, A.H., Grieve, S., Dobson-Stone, C., Kuan, S.A., Schofield, P.R., Gordon, E., Williams, L.M., 2009. Brain derived neurotrophic factor Val66Met polymorphism, the five factor model of personality and hippocampal volume: Implications for depressive illness. Hum. Brain Mapp. 30, 1246–1256.

Kambeitz, J.P., Bhattacharyya, S., Kambeitz-Ilankovic, L.M., Valli, I., Collier, D.A., McGuire, P., 2012. Effect of BDNF val(66)met polymorphism on declarative memory and its neural substrate: a meta-analysis. Neurosci. Biobehav. Rev. 36, 2165–2177.

Kennedy, K.M., Rodrigue, K.M., Land, S.J., Raz, N., 2009. BDNF val66met polymorphism influences age differences in microstructure of the corpus callosum. Front. Hum. Neurosci. 3, 19.

Kleim, J.A., Chan, S., Pringle, E., Schallert, K., Procaccio, V., Jimenez, R., Cramer, S.C., 2006. BDNF val66met polymorphism is associated with modified experience-dependent plasticity in human motor cortex. Nat. Neurosci. 9, 735–737.

Koolschijn, P.C., van Haren, N.E., Bakker, S.C., Hoogendoorn, M.L., Hulshoff Pol, H.E., Kahn, R.S., 2010. Effects of brain-derived neurotrophic factor Val66Met polymorphism on hippocampal volume change in schizophrenia. Hippocampus 20, 1010–1017.

Lang, U.E., Hellweg, R., Kalus, P., Bajbouj, M., Lenzen, K.P., Sander, T., Kunz, D., Gallinat, J., 2005. Association of a functional BDNF polymorphism and anxiety-related personality traits. Psychopharmacology (Berl) 180, 95–99.

Leemans, A., Jones, D.K., 2009. The B-matrix must be rotated when correcting for subject motion in DTI data. Magn. Reson. Med. 61, 1336–1349.

Leemans, A., Jeurissen, B., Sijbers, J., Jones, D., 2009. ExploreDTI: a Graphical Toolbox for Processing, Analyzing, and Visualizing Diffusion MR Data. ISMRM, Honolulu, USA 3536.

Liu, Y., Rutlin, M., Huang, S., Barrick, C.A., Wang, F., Jones, K.R., Tessarollo, L., Ginty, D.D., 2012. Sexually dimorphic BDNF signaling directs sensory innervation of the mammary gland. Science 338, 1357–1360.

Matsushita, S., Arai, H., Matsui, T., Yuzuriha, T., Urakami, K., Masaki, T., Higuchi, S., 2005. Brain-derived neurotrophic factor gene polymorphisms and Alzheimer's disease. J. Neural Transm. 112, 703–711.

McAllister, A.K., Katz, L.C., Lo, D.C., 1997. Opposing roles for endogenous BDNF and NT-3 in regulating cortical dendritic growth. Neuron 18, 767–778.

Molendijk, M.L., Bus, B.A., Spinhoven, P., Kaimatzoglou, A., Voshaar, R.C., Penninx, B.W., van Ijzendoorn, M.H., Elzinga, B.M., 2012. A systematic review and meta-analysis on the association between BDNF val(66) met and hippocampal volume—a genuine effect or a winners curse? Am. J. Med. Genet. B Neuropsychiatr. Genet. 159B, 731–740.

Montag, C., Weber, B., Fliessbach, K., Elger, C., Reuter, M., 2009. The BDNF Val66Met polymorphism impacts parahippocampal and amygdala volume in healthy humans: incremental support for a genetic risk factor for depression. Psychol. Med. 39, 1831–1839.

Montag, C., Basten, U., Stelzel, C., Fiebach, C.J., Reuter, M., 2010a. The BDNF Val66Met polymorphism and anxiety: support for animal knock-in studies from a genetic association study in humans. Psychiatry Res. 179, 86–90.

Montag, C., Schoene-Bake, J.C., Faber, J., Reuter, M., Weber, B., 2010b. Genetic variation on the BDNF gene is not associated with differences in white matter tracts in healthy humans measured by tract-based spatial statistics. Genes Brain Behav. 9, 886–891.

Nichols, T.E., Holmes, A.P., 2002. Nonparametric permutation tests for functional neuroimaging: a primer with examples. Hum. Brain Mapp. 15, 1–25.

Okada, T., Hashimoto, R., Numakawa, T., Iijima, Y., Kosuga, A., Tatsumi, M., Kamijima, K., Kato, T., Kunugi, H., 2006. A complex polymorphic region in the brain-derived neurotrophic factor (BDNF) gene confers susceptibility to bipolar disorder and affects transcriptional activity. Mol. Psychiatry 11, 695–703.

Pang, P.T., Lu, B., 2004. Regulation of late-phase LTP and long-term memory in normal and aging hippocampus: role of secreted proteins tPA and BDNF. Ageing Res. Rev. 3, 407–430.

Pezawas, L., Verchinski, B.A., Mattay, V.S., Callicott, J.H., Kolachana, B.S., Straub, R.E., Egan, M.F., Meyer-Lindenberg, A., Weinberger, D.R., 2004. The brain-derived neurotrophic factor val66met polymorphism and variation in human cortical morphology. J. Neurosci. 24, 10099–10102.

Pienaar, R., Fischl, B., Caviness, V., Makris, N., Grant, P.E., 2008. A methodology for analyzing curvature in the developing brain from preterm to adult. Int. J. Imaging Syst. Technol. 18, 42–68.

Ronan, L., Pienaar, R., Williams, G., Bullmore, E., Crow, T.J., Roberts, N., Jones, P.B., Suckling, J., Fletcher, P.C., 2011. Intrinsic curvature: a marker of millimeter-scale tangential cortico-cortical connectivity? Int. J. Neural Syst. 21, 351–366.

Ronan, L., Alhusaini, S., Scanlon, C., Doherty, C.P., Delanty, N., Fitzsimons, M., 2012. Widespread cortical morphologic changes in juvenile myoclonic epilepsy: evidence from structural MRI. Epilepsia 53, 651–658.

Ronan, L., Voets, N., Rua, C., Alexander-Bloch, A., Hough, M., Mackay, C., Crow, T.J., James, A., Giedd, J.N., Fletcher, P.C., 2013. Differential tangential expansion as a mechanism for cortical gyrification. Cereb. Cortex. http://dx.doi.org/10.1093/cercor/bht082 (Electronic publication ahead of print March 2013).

Schlaug, G., Armstrong, E., Schleicher, A., Zilles, K., 1993. Layer V pyramidal cells in the adult human cingulate cortex. A quantitative Golgi-study. Anat. Embryol. (Berl.) 187, 515–522.

Sen, S., Nesse, R.M., Stoltenberg, S.F., Li, S., Gleiberman, L., Chakravarti, A., Weder, A.B., Burmeister, M., 2003. A BDNF coding variant is associated with the NEO personality inventory domain neuroticism, a risk factor for depression. Neuropsychopharmacology 28, 397–401.

Shalev, I., Lerer, E., Israel, S., Uzefovsky, F., Gritsenko, I., Mankuta, D., Ebstein, R.P., Kaitz, M., 2009. BDNF Val66Met polymorphism is associated with HPA axis reactivity to psychological stress characterized by genotype and gender interactions. Psychoneuroendocrinology 34, 382–388.

Sled, J.G., Zijdenbos, A.P., Evans, A.C., 1998. A nonparametric method for automatic correction of intensity nonuniformity in MRI data. IEEE Trans. Med. Imaging 17, 87–97.

Smith, S.M., 2002. Fast robust automated brain extraction. Hum. Brain Mapp. 17, 143–155.

Smith, S.M., Jenkinson, M., Woolrich, M.W., Beckmann, C.F., Behrens, T.E., Johansen-Berg, H., Bannister, P.R., De Luca, M., Drobnjak, I., Flitney, D.E., Niazy, R.K., Saunders, J., Vickers, J., Zhang, Y., De Stefano, N., Brady, J.M., Matthews, P.M., 2004. Advances in functional and structural MR image analysis and implementation as FSL. Neuroimage 23 (Suppl. 1), S208–S219.

Smith, S.M., Jenkinson, M., Johansen-Berg, H., Rueckert, D., Nichols, T.E., Mackay, C.E., Watkins, K.E., Ciccarelli, O., Cader, M.Z., Matthews, P.M., Behrens, T.E., 2006. Tract-based spatial statistics: voxelwise analysis of multi-subject diffusion data. Neuroimage 31, 1487–1505.

Soliman, F., Glatt, C.E., Bath, K.G., Levita, L., Jones, R.M., Pattwell, S.S., Jing, D., Tottenham, N., Amso, D., Somerville, L.H., Voss, H.U., Glover, G., Ballon, D.J., Liston, C., Teslovich, T., Van Kempen, T., Lee, F.S., Casey, B.J., 2010. A genetic variant BDNF polymorphism alters extinction learning in both mouse and human. Science 327, 863–866.

Szeszko, P.R., Lipsky, R., Mentschel, C., Robinson, D., Gunduz-Bruce, H., Sevy, S., Ashtari, M., Napolitano, B., Bilder, R.M., Kane, J.M., Goldman, D., Malhotra, A.K., 2005. Brain-derived neurotrophic factor val66met polymorphism and volume of the hippocampal formation. Mol. Psychiatry 10, 631–636.

Takahashi, T., Suzuki, M., Tsunoda, M., Kawamura, Y., Takahashi, N., Tsuneki, H., Kawasaki, Y., Zhou, S.Y., Kobayashi, S., Sasaoka, T., Seto, H., Kurachi, M., Ozaki, N., 2008. Association between the brain-derived neurotrophic factor Val66Met polymorphism and brain morphology in a Japanese sample of schizophrenia and healthy comparisons. Neurosci. Lett. 435, 34–39.

Teo, J.T.H., Bentley, G., Lawrence, P., Soltesz, F., Miller, S., Willé, D., McHugh, S., Dodds, C., Lu, B., Croft, R.J., Bullmore, E.T., Nathan, P.J., 2014. Late cortical plasticity in motor and auditory cortex: role of met-allele in BDNF val66met polymorphism. Int. J. Neuropsychopharmacol. (in press).

Toro, R., Chupin, M., Garnero, L., Leonard, G., Perron, M., Pike, B., Pitiot, A., Richer, L., Veillette, S., Pausova, Z., Paus, T., 2009. Brain volumes and Val66Met polymorphism of the BDNF gene: local or global effects? Brain Struct. Funct. 213, 501–509.

Tost, H., Alam, T., Geramita, M., Rebsch, C., Kolachana, B., Dickinson, D., Verchinski, B.A., Lemaitre, H., Barnett, A.S., Trampush, J.W., Weinberger, D.R., Marenco, S., 2013. Effects of the BDNF Val66Met polymorphism on white matter microstructure in healthy adults. Neuropsychopharmacology 38, 525–532.

Tournier, J.D., Calamante, F., Connelly, A., 2007. Robust determination of the fibre orientation distribution in diffusion MRI: non-negativity constrained super-resolved spherical deconvolution. Neuroimage 35, 1459–1472.

Tournier, J.D., Mori, S., Leemans, A., 2011. Diffusion tensor imaging and beyond. Magn. Reson. Med. 65, 1532–1556.

Tzourio-Mazoyer, N., Landeau, B., Papathanassiou, D., Crivello, F., Etard, O., Delcroix, N., Mazoyer, B., Joliot, M., 2002. Automated anatomical labeling of activations in SPM using a macroscopic anatomical parcellation of the MNI MRI single-subject brain. Neuroimage 15, 273–289.

Ventriglia, M., Bocchio Chiavetto, L., Benussi, L., Binetti, G., Zanetti, O., Riva, M.A., Gennarelli, M., 2002. Association between the BDNF 196 A/G polymorphism and sporadic Alzheimer's disease. Mol. Psychiatry 7, 136–137.

Verhagen, M., van der Meij, A., van Deurzen, P.A., Janzing, J.G., Arias-Vasquez, A., Buitelaar, J.K., Franke, B., 2010. Meta-analysis of the BDNF Val66Met polymorphism in major depressive disorder: effects of gender and ethnicity. Mol. Psychiatry 15, 260–271.

Voineskos, A.N., Lerch, J.P., Felsky, D., Shaikh, S., Rajji, T.K., Miranda, D., Lobaugh, N.J., Mulsant, B.H., Pollock, B.G., Kennedy, J.L., 2011. The brain-derived neurotrophic factor Val66Met polymorphism and prediction of neural risk for Alzheimer disease. Arch. Gen. Psychiatry 68, 198–206.

Vos, S.B., Jones, D.K., Viergever, M.A., Leemans, A., 2011. Partial volume effect as a hidden covariate in DTI analyses. Neuroimage 55, 1566–1576.

Wakana, S., Caprihan, A., Panzenboeck, M.M., Fallon, J.H., Perry, M., Gollub, R.L., Hua, K., Zhang, J., Jiang, H., Dubey, P., Blitz, A., van Zijl, P., Mori, S., 2007. Reproducibility of quantitative tractography methods applied to cerebral white matter. Neuroimage 36, 630–644.

Welker, W., 1990. Why does the cerebral cortex fissure and fold? A review of determinants of gyri and sulci. In: Jones, E.G., Peters, A. (Eds.), Cerebral Cortex. Springer, US, pp. 3–136.